Measuring surface currents with Surface Velocity Program drifters: the instrument, its data, and some recent results

RICK LUMPKIN AND MAYRA PAZOS
National Oceanographic and Atmospheric Administration,
Atlantic Oceanographic and Meteorological Laboratory, Miami, FL USA

Chapter two of "Lagrangian Analysis and Prediction of Coastal and Ocean Dynamics," ed. A. Mariano, T. Rossby and D. Kirwan, Cambridge Univ. Press

1. Introduction

For centuries, our knowledge of the oceans' surface circulation was inferred from the drift of floating objects. Dramatic examples include wrecked Chinese junks and Japanese glass fishing balls which have washed ashore on the US west coast (Sverdrup et al., 1942). Such observations could only provide crude ideas of gyre-scale currents, as there was no way to tell the exact beginning (in time or space) of the drifter's journey, or the trajectory it had taken. Currents can be more accurately inferred from ship drift measurements. A ship's motion relative to the surrounding water is measured by the ship log; its absolute motion is estimated from navigational fixes. In the absence of wind and the "sailing" force of flow around the hull and keel, the difference between absolute and relative motion is the velocity of the water (the current). However, due to relatively large navigational errors in the mostly pre-GPS data set of ship drifts, such current estimates can have errors of O(20 cm/s) (Richardson and McKee, 1984). In addition, a drifting ship is exposed to both currents and wind, making the relative role of the two forces difficult to separate. Comparison of ship drifts with less windage-prone measurements have revealed significant differences in the tropical Pacific (Reverdin et al., 1994) and Atlantic (Richardson and Walsh, 1986; Lumpkin and Garzoli, 2005). To reduce the wind force, investigators in the early 1800s began using drift-bottles to map surface currents. These bottles were typically weighed down so that they were almost entirely submersed, and typically carried a note indicating their launch location and time (Sverdrup et al., 1942). Bottles have been used to map currents in regions such as the North Sea (Fulton, 1897; Tait, 1930) and northwestern Pacific Ocean (Uda, 1935).

A major step towards collecting true Lagrangian time series of velocity was made by attaching a sea anchor, or "drogue", to a buoyant object that would not extend far above the surface but could be tracked by triangulation from a fixed point (such as an anchored ship). Observations of this nature were collected off the US east coast as early as the mid-1700s (Franklin, 1785; Davis, 1991) and were collected worldwide in the famous 1872–1876 *Challenger* oceanographic survey at most of the 354 hydrographic stations (Thomson, 1877; Niiler, 2001). With the advent of radio, drifter positions could be transmitted from small, low-drag antennae and triangulated from shore (Davis, 1991). Drifters of this type are still manufactured today, often inspired by the cruciform-shaped design used in the Coastal Ocean Dynamics Experiment (CODE). In CODE, 164 drifters were used to map currents and their variability and to calculate Lagrangian integral scales and dispersion off the California coast (Davis, 1985).

The early 1970s saw the introduction of positioning via satellite observations of an earthbound transmitter's Doppler shift. This was first done using the NIMBUS satellites and later the more accurate Argos Data Collection and Location System carried aboard the National Oceanic and Atmospheric Administration (NOAA) TIROS-N polar-orbiting satellites. Several independent groups promptly developed and deployed satellite-tracked surface drifting buoys. One of the earliest such deployments was in 1975 as part of the North Pacific Experiment (NORPAX). NORPAX drifters were 3 m long, 38 cm-diameter fiberglass cylinders, drogued at 30 m with a 9 m parachute (McNally et al., 1983). An array of 35 drifters, drogued with 200 m of polypropylene line and either a 25 kg weight or a windowshade sail, was deployed in the Gulf Stream region in 1976-1978 (Richardson, 1980). These drifters included a tether strain sensor to indicate drogue status, but this sensor frequently failed shortly after deployment. A large array of over 300 Argos-tracked drifters was deployed as part of the Global Atmosphere Research Program (GARP) First Global GARP Experiment (FGGE) in 1979–80 in the Southern Ocean (Garrett, 1980). FGGE drifters were configured in various designs, with the "regular" variety having a tall (3.4 m) surface float and 100 m line acting as a drogue, weighted at the end with 29.5 kg of chain. Other FGGE drifters had large vanes for measuring wind direction. From 1981–84, 113 HERMES-type drifters, drogued with a windowshade sail at 100 m depth, were deployed in the eastern and northern North Atlantic (Krauss and Böning, 1987). In 1983–85, 53 TIROS and mini-TIROS drifters were deployed in the tropical Atlantic as part of the SEQUAL (Seasonal Response of the Equatorial Atlantic) and FOCAL (Programme Francaise Océan-Climat en Atlantique Equatorial) programs. The TIROS design had a windowshade drogue of area 20 m^2 centered at 20 m depth, while the mini-TIROS had a 2.2 m^2 windowshade centered at 5 m depth (Richardson and Reverdin, 1987). The drifters did not have sensors to indicate drogue presence, although two TIROS drifters recovered after 217 days at sea had drogues in "excellent condition" (Richardson and Reverdin, 1987).

2. The SVP drifter

In 1982 the World Climate Research Program (WCRP) recognized that a global array of drifters would be invaluable for oceanographic and climate research, but uncertainties and large variations in the water following properties of various drifter designs posed a major challenge, along with the high costs and excessive weight of some drifter types (World Climate Research Program, 1988; Niiler, 2001). The WCRP declared that a standardized, low-cost, lightweight, easily-deployed surface drifter should be developed, with a semi-rigid drogue which would maintain its shape in high-shear flows. This development took place under the Surface Velocity Program (SVP) of the Tropical Ocean Global Atmosphere (TOGA) experiment and the World Ocean Circulation Experiment (WOCE). Initial funding was provided by the US Office of Naval Research, with subsequent support from NOAA and the National Science Foundation. Competing designs were submitted by NOAA's Atlantic Oceanographic and Meteorological Laboratory (AOML), MIT's Draper Laboratory, and Scripps Institution of Oceanography (SIO) (Niiler, 2003).

During the 1980s these designs continued to evolve, and in 1985–89 they were rigorously evaluated on a number of criteria including their water-following characteristics, quantified by attaching vector-measuring current meters to the tops and bottom of the drogues (Niiler et al., 1987, 1995). Several drogue designs were examined and various problems identified. For example, windowshade drogues could twist and sail across a current; parachute drogues could collapse and subsequently provide very little drag; the line-and-chain FGGE drogue provided too little area compared to the surface float, resulting in significant slip with respect to the currents at the drogue depth (Niiler et al., 1987, 1995; Niiler and Paduan, 1995; Pazan and Niiler, 2001). Other factors were also considered; for example the rigid three-dimensional tristar drogue was found to have somewhat better water-following characterists than the holey-sock drogue developed at AOML, but the increased manufacturing and shipping costs and more difficult deployments for the tristar outweighted this benefit. By 1993 a clear design for the SVP drifter had emerged which combined the holey-sock drogue of the AOML drifters with reinforced tether ends and surface float designs from SIO. This design (Sybrandy and Niiler, 1992) became the foundation for future SVP drifter development.

The modern data set of "SVP" drifters includes all drifters deployed during the 1979–1993 development period that had a holey-sock drogue centered at 15 m depth. AOML spar-type drifters with holey-sock drogues were first deployed in February 1979 as part of the TOGA/Equatorial Pacific Ocean Circulation Experiment (EPOCS). Large-scale deployments of the first modern SVP drifters took place in 1988 (World Climate Research Program, 1988) with the goal of mapping the tropical Pacific Ocean's surface circulation. This effort was expanded to global scale as part of WOCE and the Atlantic Climate Change Program (ACCP), in which the array of SVP drifters was extended to cover the Pacific and North Atlantic Oceans by 1992 and the Southern and Indian Oceans by 1994 (Niiler, 2001). The array spanned the tropical and South Atlantic Ocean by 2004 (Lumpkin and Garzoli, 2005).

Today the array of SVP drifters is known collectively as the Global Drifter Program (GDP), a component of NOAA's Global Ocean Observing System (GOOS) and Global Climate Observing System (GCOS) and a scientific project of the Data Buoy Cooperation Panel (DBCP) of the World Meteorological Organization and International Oceanographic Commission. The scientific objectives of the GDP are to provide operational, near-real time surface velocity, sea surface temperature (SST) and sea level pressure observations for numerical weather forecasting, research, and in-situ calibration/verification of satellite observations. The GDP is managed in close cooperation between NOAA/AOML in Miami, Florida, NOAA/SIO's Joint Institute of Marine Observations (JIMO) in La Jolla, California, and three private US drifter manufacturers (Clearwater, Pacific Gyre and Technocean). AOML arranges and conducts drifter deployments, processes the data, maintains files which describe each drifter, and hosts the GDP website (www.aoml.noaa.gov/phod/dac) JIMO supervises the industry, acquires the drifters from the various manufacturers, upgrades the technology, develops new sensors, and creates enhanced data sets (Pazan and Niiler, 2004) to the research community. The manufacturers build the SVP drifters according to closely-monitored specifications.

a. Design

At present, there are two basic sizes of SVP drifters: the original, relatively large SVP drifter and the new "mini" version (Fig. 1). The original design is extremely robust but is relatively expensive and heavy. A more gracile redesign was proposed in DBCP Specification Rev. 1.2 in December 2002. This "mini" drifter is produced alongside SVP drifters of original dimensions by several manufacturers. Present manufacturers of SVP drifters include Clearwater Instrumentation (Watertown, MA USA; www.clearwater-inst.com), Marlin-Yug (Sevastopol, Ukraine; marlin.stel.sebastopol.ua), Metocean Data Systems (Dartmouth, Nova Scotia, Canada; www.metocean.com), Pacific Gyre (Oceanside, CA USA; www.pacificgyre.com), and Technocean (Cape Coral, FL USA; www.technocean.com).

The surface float of an SVP drifter ranges from 30.5 cm (the smallest mini) to 40 cm in diameter. Originally, the surface float hull was made of 0.3–0.4 cm-thick fiberglass (thicker at the tether protrusion; c.f. Sybrandy and Niiler 1991, Fig. 3). Most manufacturers have now switched to less expensive ABS (Acrylonitrile-Butadiene-Styrene) plastic for surface float hull construction. The surface float contains: batteries in diode-protected packs, typically 4–5 packs each with 7–9 alkaline D-cell batteries; a satellite transmitter (401.650 MHz, $\pm$ 10 kHz) typically activated by removing a magnet from the float hull; a thermistor for sub-skin sea surface temperature, located at the base of the float to avoid direct radiative heating; and possibly other instruments measuring barometric pressure, wind speed and direction, salinity, or ocean color. Most surface floats also include a submergence sensor, consisting of two screws extruding from the hull. This sensor is used to identify the presence of the drogue, which frequently drags the surface float beneath the sea surface – an abrupt drop in the percentage of submerged time indicates that the drogue has been lost. One manufacturer (Clearwater) has replaced the submergence sensor with a tether strain sensor, which more directly measures drogue presence. Most manufacturers apply cuprous oxide paint to the bottom half of the surface float to reduce biofouling. A polypropylene-impregnated wire rope tether connects the surface float to a subsurface float (original design; 5.6 mm diameter tether) or directly to the drogue (mini drifter, with a 3.2 mm diameter tether).

An SVP drifter has its drogue centered at 15 m depth to measure mixed layer currents; other options (such as 100 m) have been made available to individual researchers. The outer surface of the drogue is Cordura nylon cloth.

In the original design, it is composed of 7 sections, each 92 cm long and 92 cm in diameter for a total length of 6.44 m. Mini drogues are not yet standardized among the manufacturers: they are composed of 4 (Pacific Gyre) or 5 (Marlin-Yug) sections of original dimensions, or 4 (Clearwater) or 5 (Technocean) redesigned sections of diameter 61 cm, length 1.22 m/section. Throughout the drogue, PVC or polypropylene pipe rings with wire rope spokes provide support, maintaining the drogue's cylindrical shape. The top ring is filled with polyurethane foam to provide some positive buoyancy, reducing accordion-type oscillations when tether strain is low (Sybrandy and Niiler, 1992). Lead weights (in some drifters, sand ballast in a polypropylene pipe) sewn into the base of the drogue insure that it hangs nearly vertically. The drogue is a "holey-sock," i.e. each drogue section contains two 46 cm (mini: 30 cm) diameter opposing holes, which are rotated 90° from one section to the next (see Fig. 1). These holes act like the dimples of a golf ball by disrupting the otherwise laminar flow which would generate organized lee vortices. As a consequence, the drogue does not experience an abrupt change in drag coefficient across a critical Reynolds number which would be associated with vortex shedding (Nath, 1977).

While the sizes of the surface float and drogue vary, the manufacturers all aim for a specific nondimensional goal: a drag area ratio of $\sim$40. This ratio is the drag area (drag coefficient times cross-sectional area) of the drogue, divided by the drag area of all other components. At a drag area ratio of 40, the resulting downwind slip (see Section **4.**a.) is 0.7 cm/s in 10 m/s winds; for comparison, a standard FGGE-type drifter had a drag area ratio of 10–12 and a downwind slip of 8 cm/s in 10 m/s winds (Niiler and Paduan, 1995; Pazan and Niiler, 2001). In practice, the manufacturer-provided drag area ratios range from 37.5–45.9. Some modified drifters include substantial additional components which greatly reduce the drag area ratio. An example is Marlin-Yug's SVP-BTC drifter which has a thermistor chain extending to 60 m depth, reducing the drag area ratio to 6.8.

b. Deployment

Original-sized SVP drifters are packaged two per cardboard box of dimension 1.07 m (3'6") cubed. Each drifter weights approximately 45 kg (100 lbs) and can be deployed by a single person, although in heavy seas it is recommended that two people deploy an original SVP drifter. Mini drifters are packaged five per cardboard box of the same dimensions, or two in a box of size 1.17×0.89×0.56 m. The mini weighs approximately 20 kg (44 lbs) and can easily be deployed by one person. The drogue and tether are bound with paper tape which dissolves in the water, and the tether is sometimes wrapped around a water-soluble cardboard tube to protect it from kinking. The drifter is deployed by throwing it from the stern of a vessel, preferably from the lowest deck and within 10 m of the sea surface. The ship may be underway; successful deployments have been conducted from cargo ships steaming at up to 25 knots. After deployment, it may take approximately an hour for the drogue to become fully soaked, allowing the paper tape to dissolve and trapped air bubbles to be released, before the drogue sinks.

Drifters have also been air-deployed out of Lockheed C-130 Hercules, operated by the Air Force Reserve "Hurricane Hunters" (53d Weather Reconnaissance Squadron, 403d Wing, Keesler Air Force Base), and by the Naval Oceanographic Office (NAVOCEANO) which conducts surveys supporting naval operations primarily in the northern hemisphere. Deployments have also been conducted from a C-141 Starlifter. Air deployment requires extensive rigging of the drifter package, including adding the parachute, at a cost approximately equal to the drifter itself (P. Niiler, pers. comm.).

During the one-year period September 2003–August 2004, a total of 658 drifters were deployed in NOAA's contribution to the Global Drifter Program. Of these, 440 were deployed off research vessels, 201 off volunteer observation ships (typically cargo vessels), and 17 were air-deployed.

c. Data transmission

Drifter sensor data (including SST and battery voltage) are typically sampled at intervals of 90 s. Averages are calculated over an observation cycle of seven to ten samples and transmitted. Submergence or strain data transmission varies by manufacturer. For example, Metocean drifters sample the submergence four times every 90 s, and sum the total number of underwater samples over a 30 minute averaging period to determine the percentage of time submerged. The data are formatted for transmission with checksum entries provided in a 32-bit Argos (see below) message. Older drifters often used a duty cycle of 1/3 (typically the transmitter spent one day on, then two days off), which could lead to significant biasing of high latitude inertial motion (Bograd et al., 1999). Nearly all drifters since 2001 operate on a 100% duty cycle. Recently-developed drifters exploit multiplexing techniques to increase data transmission. During one satellite pass, 6–7 data frames can be sent every 90 s, or twice this many with a 45 s repetition rate. Each transmitter is assigned a Platform Terminal Transmitter (PTT) code by Argos, often referred to as the drifter ID number.

Argos (http://www.argosinc.com/) is an American-French satellite-based system for collecting, processing and distributing data. It is operated by Collecte Localisation Satellites (CLS) in Toulouse, France, with a subsidiary (Service Argos, Inc.) in Largo, Maryland USA. Since 1978, the Argos system has been carried on the US National Oceanographic and Atmospheric Administration (NOAA) Polar Orbiting Environmental Satellites to obtain global coverage. In addition, a second-generation Argos system was carried aboard the Japanese Advanced Earth Observing Satellite II (ADEOS-II), launched in December 2002. This joint Argos/ADEOS-II program ("Argos Next") was declared operational on 5 May 2003; unfortunately, the satellite failed on 25 October 2003. Future launches with next-generation Argos systems are planned aboard the European METOP satellites, beginning in the last quarter of 2005.

The position of a drifter is inferred from the Doppler shift of its transmission. The position-deducing algorithm can be summarized as follows (Argos, 1996). As the satellite approaches, passes and recedes from the latitude of a drifter, the satellite's speed (7.4 km/s) Doppler shifts the signal. The timing of the swing from blue to red (but not exactly the latitude of the shift, due to drifter motion; see below) gives the drifter's latitude, and the rapidness of the swing gives the off-track direction (the closer the satellite pass is to the drifter, the more step-like the swing). The absolute motion of the drifter introduces an additional Doppler shift: at 20°N, a fixed point on the Earth's surface travels 437 m/s westward. Thus, if the drifter is east of the satellite pass, an additional blue shift is superimposed which reaches its maximum as the satellite crosses the drifter's latitude. This Doppler shift decays with increased distance from the drifter at a rate dependent upon the minimum satellite/drifter distance (greater distance equals slower decay). The sign of this shift is estimated from least-squares fitting and the previous history of the drifter, and gives the off-track direction.

Argos estimates the accuracy of position fixes at 150–1000 m. The largest errors occur when a satellite pass is close to, but not directly over, a drifter. In this situation the Doppler shift from the absolute drifter motion is a relatively brief spike which can be difficult to resolve – possibly causing the Argos position algorithm to "place" the drifter on the wrong side of the pass. When this happens, there are relatively large errors in longitude, with much smaller latitudinal errors. Additional errors can arise due to satellite instrumental noise and inaccuracies in orbit and time coding (Hansen and Poulain, 1996). From a 70 day time series of position fixes for a grounded drifter in Honolulu, Hawaii, we have calculated the root-mean-square error in a fix to be 630 m zonally, 270 m meridionally. This drifter's transmitter was not held ridgidly vertical, possibly introducing a bias to some of the satellite fixes (J. Wingenroth, pers. comm.) that would not be experienced by a drogued drifter in the water. The 70-day median of the Argos fixes was not significantly different from a GPS fix.

d. Drifter lifetime

The manufacturers' estimate for an original SVP drifter lifetime is ∼400 days. In order to examine the accuracy of this claim, we have calculated the half life for SVP drifters deployed in 1998–2003. This was calculated for all drifters which had not run aground or been picked up by boaters. The remaining drifters were sorted by the year in which they had been deployed. For each year's batch of drifters, we calculated how many days of observations were obtained, and how many days of drogued observations were obtained. Drifters still transmitting (and still drogued, for the drogue half life) were assigned a large placeholder value (9999 days). The histogram of these lifetimes was used to identify the amount of time after which one-half of the drifters were no longer alive, and after which one-half were no longer providing drogued velocity observations. The half lives are shown in Fig. 2. Transmitter lifetimes generally increased during 1998–2002, from 291 days in 1998 to 400 days in 2002, with a peak of 485 days in 2001. These calculations do not include drifters which failed to transmit upon deployment: 12% of drifters in 1998, 5% in 2001 and 3% in 2003. More than half the drifters deployed in 2003 were still alive and drogued at the time of this writing (November 2004), making their half life impossible to determine; given the temporal distribution of deployments through 2003 and the histogram of lifetimes so far, it is likely to exceed 450 days.

Thus, while some individual batches of drifters have had a high failure rate due to causes ranging from defects during manufacturing to deployment in extremely harsh conditions (e.g., air-deployed in the path of a hurricane), the general tendency across recent years is encouraging. In addition to the development of the mini drifter described earlier, incremental improvements in drogue reinforcement, tether/drogue attachment, and transmitter design are successfully increasing the value of the SVP drifter. At the same time, the cost of a drifter has steadily dropped, from USD 5475 in 1993 (adjusted to 2003 US dollars; Niiler, 2003) to USD 1750 today.

3. Drifter data: Quality control, interpolation and coverage

Before December 2004, position fixes acquired by two of the satellites were processed by Argos. For a typical drifter near the equator, 6–9 fixes per day were acquired. At higher latitudes the polar-orbiting satellite passes were closer, yielding 8–10 fixes per day at 20° latitude. The theoretical maximum was 28 fixes per day at the poles (Argos, 1996). In late 2004 the Joint Tariff Agreement (see www.ogp.noaa.gov/argos/overview.htm) negotiated the use of the full satellite constellation (up to four at present). Since mid-December 2004, this "multi-satellite service" has been yielding 16–20 fixes per day for equatorial drifters. AOML's Drifting Buoy Data Assembly Center (DAC; www.aoml.noaa.gov/phod/dac/dac.html) assembles these raw data, applies quality control procedures, and interpolates them to regular 1/4-day intervals. The raw observations and processed data are archived at AOML's DAC and at Canada's Marine Environmental Data Service (MEDS; www.meds-sdmm.dfo-mpo.gc.ca).

a. Quality control

The DAC first visually examines drifter data for evidence that the data were transmitted while on the deck of a ship, the drifter was aground, or the drifter has been picked up by a boater. These drifters are usually apparent from their trajectories, and can be supported by submergence values and the diurnal variations in temperature. These observations are removed from the data set.

Next, the DAC identifies drifters which have lost their drogues. This is done using the submergence or tether strain observations. The drogue lost dates are compiled in a "directory file" which includes each drifter's deployment time and location, ending time and location, and the type of death (e.g., picked up, ran aground, stopped transmitting). These dates are stored using a modified Julian day convention in which day 1 is January 1, 1979. For a drifter that never lost its drogue, the directory file holds the placeholder value 0 for drogue off time while it is still alive (still transmitting good data), or the date of its final reliable transmission if it has died.

To eliminate the more egregious errors in raw Argos fixes, the DAC applies a two-step quality control scheme (Hansen and Poulain, 1996). In this methodology, the velocity is calculated via finite differencing of the raw fixes both forward and backward in time. A fix is flagged as "bad" if it produces a velocity greater than four standard deviations from the mean velocity in both forward and backward passes. Two-way differencing is used because a forward-only calculation may fail to identify a bad fix if it comes immediately after a gap in data acquisition.

b. Interpolation

The raw fixes are interpolated to uniform 6-h intervals using an optimal interpolation procedure known as kriging (Hansen and Herman, 1989; Hansen and Poulain, 1996). Latitude and longitude (and SST) are interpolated independently. Kriging assumes that the observations consist of a "true" signal contaminated by noise, the latter assumed to be white and unbiased (zero mean). Interpolated values are constructed by a linear combination of the five observations preceding and five following the interpolation point (if available), using a set of weights constructed such that the root-mean-square difference between the true value and the concurrent interpolated value is minimized.

In the kriging procedure, the (true) position is described by a structure function. For this, Hansen and Poulain (1996) used a fractional Brownian model that can describe motion ranging from uncorrelated Brownian diffusion to perfectly correlated linear advection. They estimated the parameters for the model using tropical Pacific Ocean drifter observations for the period 1988-1993. The resulting parameters yielded a model which was a blend of advection and diffusion, with advection more significant for zonal displacements. This result is consistent with studies which have found strong anisotropy in the zonal vs. meridional scales of dispersion in the tropics, with much longer zonal integral length scales (e.g., Lumpkin and Flament, 2001). This model is probably not the most appropriate choice at higher latitudes away from strong zonal currents.

Along with the interpolated positions, AOML provides formal error bars on the positions. These can be invaluable in identifying large gaps – as long as two weeks – across which the data have been interpolated, as these will have large error bars. Researchers working with the drifter data should approach these data with caution; they may be useful for calculating mean advective pathways, but should not be included in calculations of eddy kinetic energy or dispersion (see Fig. 3).

Following interpolation, the zonal and meridional components of velocity are calculated via centered finite differencing over 1/2 day displacements. Many investigators interested in subinertial motion (e.g., Ralph and Niiler, 1999; Fratantoni, 2001; Lumpkin and Garzoli, 2005) apply a lowpass filter to these velocities before proceeding with their analyses.

c. Data coverage

SVP drifter observations now cover most areas of the world's oceans at sufficient density to map mean currents at 1° resolution (Fig. 4).

The recent growth of the drifter array is shown in Fig. 5. The number of drifters in the global array has increased tremendously due to the efforts of many individual investigators and international partnerships contributing to the Global Ocean Observing System (GOOS). The GOOS goal of maintaining a 5° by 5° network of drifters will require 1250 drifters, and is anticipated to be achieved in September 2005. As of November 2004, the global array has reached 1100 drifters. From 1998 to 2003, drifter coverage has increased in all basins shown in Fig. 5 except the North Pacific. Recent air deployments by NAVOCEANO south of the Aleutian Islands, along with future deployments from volunteer observation ships running the great circle route between Japan and California, are addressing this gap.

4. Velocity observations

Fig. 4 shows time-mean surface currents (middle) and eddy kinetic energy (bottom) for the world's oceans, calculated on a 1° by 1° grid via Gauss-Markov decomposition (Lumpkin, 2003). Annual and semiannual amplitudes and phases (not shown) were calculated at the same resolution. All of the major western boundary currents (Gulf Stream, Philippines/Kuroshio, Brazil, North Brazil, East Australian, Mozambique/Agulhas and Somali) are clearly seen as maxima in both mean current speed and eddy energy. The time-mean zonal structure of tropical currents such as the northern South Equatorial Current and North Equatorial Countercurrent are prominent features of Fig. 4, as are the monsoon-driven semiannual currents of the equatorial Indian Ocean.

SVP drifters provide imperfect pseudo-Lagrangian observations at the drogue depth – "pseudo" because water parcels can upwell or downwell while the drifter stays at the surface, and imperfect because of slip (see below). The resulting observations of mixed layer velocity are thus a combination of slip, plus the directly wind-driven flow in the upper mixed layer, plus the 15 m-deep signature of the underlying eddy and gyre-scale currents. Time-mean plots of these components, derived from National Centers for Environmental Prediction (NCEP) Reanalysis Ver. 2 winds and the parameterizations described below, are shown in Fig. 6.

a. Slip, with and without a drogue

Slip is the horizontal motion of a drifter that differs from the lateral motion of currents averaged over the drdogue depth. Slip is caused by direct wind forcing on the surface float, drag on the float and tether induced by wind-driven shear, and surface gravity wave rectification (Niiler et al., 1987; Geyer, 1989). In order to reduce wave rectification, the surface float is spherical (Niiler et al., 1987, 1995). The original SVP design included a 20 cm diameter subsurface float between the surface float and drogue, intended to decouple their motion and to provide additional buoyancy offsetting the weighted drogue. The subsurface float has been omitted in the recent mini drifter redesign. The most important design characteristics that minimize slip are low tension between the surface buoy and drogue, which avoids aliasing wave motion, and a large drag area ratio (Niiler et al., 1987). As long as the drogue remains attached to the drifter, the downwind slip is estimated at 0.7 cm/s per 10 m/s of wind speed (Niiler and Paduan, 1995).

Pazan and Niiler (2001) examined a data set of 2334 SVP drifters, including 1845 which had lost their drogues while continuing to transmit location. They examined residual (undrogued minus drogued) drifter motion using a multiple regression model with local surface wave height (from the Fleet Numerical Meteorology and Oceanography Center, FNMOC) and winds (FNMOC, NCEP, and the European Center for Medium range Weather Forecasting, ECMWF). The residual motion did not have a significant relationship with waves, either because wave drift is negligible or because the relationship is obscured by errors in or resolution of the wave data set. Residual motion was aligned on average directly downwind, and was linearly dependent upon wind velocity with a global mean value of 7.9$\pm$0.7 cm/s per 10 m/s of wind. This result and those of Niiler and Paduan (1995) indicate that an undrogued SVP drifter experiences a slip of 8.6$\pm$0.7 cm/s per 10 m/s wind.

b. Ekman drift

Niiler and Paduan (1995) analyzed the Lagrangian velocity time series of 8 drogued SVP drifters in the northeast Pacific during October 1989–April 1990. They found that velocity and local wind (using 6-hourly ECMWF operational winds) was highly coherent at subinertial periods of 5–20 days. At shorter periods inertial oscillations dominated the Lagrangian velocity spectra, while at longer periods mesoscale variations (uncorrelated with local wind) dominated the spectra. The 5–20 day bandpassed velocity was 60–100° to the right of the wind, consistent with Ekman dynamics. For the bandpassed velocities and winds, Niiler and Paduan derived the linear regression model $\boldsymbol{U} = b\boldsymbol{\tau}_o$, where τ_o is the wind stress at the ocean surface, $\boldsymbol{U} = u + iv$, (u, v) are the zonal and meridional components of velocity, $i = \sqrt{-1}$ and the complex coefficient b has amplitude $|b|$=0.28 m (s Pa)$^{-1}$ and angle 77° to the right of the wind. This model accounted for 35% of the variance in the bandpassed drifter velocities.

In a study of 1503 SVP drifters in the tropical Pacific 20°S–20°N, 1988-1996, Ralph and Niiler (1999) removed the time-mean geostrophic motion using the hydrographic climatologies of Levitus (1982) and Kessler and Taft (1987). They averaged the residual velocities in 2° by 5° bins and examined various models regressing this velocity onto concurrent, interpolated 6-hourly winds from operational ECMWF. Niiler (2001) repeated this calculation with a larger data set (30°S–30°N, 1988-1999) using NCEP reanalysis winds. These studies found that 49% of the variance across the bins could be accounted for by the model $U = Au^*/f^{1/2}$, where U is the magnitude of the residual

(Ekman) velocity, $u^* = \sqrt{|\tau_o|/\rho}$ is the friction velocity due to the time-mean surface wind stress τ_o, ρ is density, f is the Coriolis parameter, and the best-fit coefficient A=(0.081±0.013) s$^{-1/2}$. The orientation of the Ekman velocity depended upon the ratio of the drogue depth d =15 m to the Ekman layer depth scale $D = u^*/A$, which varied from bin to bin. When Ralph and Niiler (1999) plotted the off-wind angle as a function of d/D they found a clockwise-rotating (in the northern hemisphere) spiral consistent with the theory of Ekman (1905).

More recently Rio and Hernandez (2003) subtracted time-mean geostrophic currents and altimetry-derived geostrophic current anomalies from concurrent drifter velocities over the globe for the period 1993–1999, to examine the wind-driven ageostrophic motion. They found that the time-varying geostrophic component was significant at periods greater than 10 days in the latitude band 15–30° (north and south), and at periods greater than four days at 30–90°. At higher frequencies drifter velocities are predominantly ageostrophic, with clear peaks in the anticyclonic spectra at inertial and tidal frequencies. The ageostrophic motion is significantly coherent with the wind in the band between 20 days and the inertial/tidal periods. By separately examining summer and winter months, Rio and Hernandez (2003) showed that the Ekman depth (parameterized as in Ralph and Niiler, 1999) varies with the seasonal change of wind speed over much of the world's subtropical and subpolar basins.

5. Other observations

The focus of this chapter is on the velocity observations made by SVP drifters. However, this platform is capable of collecting many other types of observations, some of which can be combined with velocity to estimate heat advection, ground-truth satellite-based products, and many other uses. Thus, a brief overview of these observations is warranted.

Sea surface temperature (SST): All standard SVP drifters measure temperature 20–30 cm beneath the sea surface. These data are disseminated on the Global Telecommunication System (GTS) by Argos within two hours of reception for use in numerical weather forecasting and operational SST analysis, and for calibrating SST products (c.f. Reynolds et al., 2002).

Barometric pressure: Many drifters, known as SVP-Bs, have been outfitted with a barometer to measure air pressure. Large-scale experimental deployments began in 1994; operational barometric observations have been collected since 1997. These data are particularly valuable in numerical weather prediction at high latitudes, where few in-situ observations are available if a storm develops outside the major shipping lanes. The barometer port extends ∼20 cm above the top of the surface float to minimize spuriously high spikes in the pressure record associated with submergence.

Wind: some drifters include a hydrophone for noise level, which can be converted to wind speed and precipitation estimates, and a 25 cm-by-20 cm wind vane mounted to the barometer port of the surface float (with accompanying two-axis tilt sensor in the float, and swivel connection for the tether) to measure wind direction. SVP drifters of this type are known as Minimets (Milliff et al., 2003). The WOTAN hydrophone is typically mounted either on the tether, at a depth of 11 m, or between the tether and drogue top. Recent air deployments of these drifters in the path of Category 4 Hurricane Fabian have demonstrated the ability to measure the wind direction to within $\pm 10^\circ$ (Niiler et al., 2004b), mapping the circulation of the hurricane more clearly than in QuickSCAT data, although the hydrophone became saturated at such extreme wind speeds.

Ocean color: Some drifters have included an upwelling radiance sensor mounted on the surface float just beneath the sea surface, along with a downwelling irradiance sensor. Their observations have been used to study chlorophyll variations in remote regions such as the Southern Ocean (Letelier et al., 1996).

Salinity: The first salinity-measuring drifters were developed at Scripps Institution of Oceanography (SIO) by attaching a SeaBird SeaCat (thermistor and conductivity) to the top of the drogue (11 m depth). In 1992-3, 72 of these drifters were deployed in the tropical Pacific and provided observations which compared favorably to the TAO mooring data (Kennan et al., 1998). Four of these drifters were recovered after 310 days at sea, with post-calibration revealing a maximum offset of 0.02 psu.

More recently, drifters have been developed which can measure surface salinity. At SIO, SeaBird Microcats have been mounted to the base of the surface float. Parallel development is being conducted at Woods Hole Oceanographic Institution. Thirty of the SIO drifters were deployed in the East China Sea in the period 2000-2004, to help evaluate the effects of the decreasing Yangzte flow on the ecology of South Korea. Two were recovered several weeks after deployment, and showed no detectable offset when post-calibrated (P. Niiler, pers. comm.).

Biofouling presents the major challenge to obtaining extended observations of surface salinity. Ongoing experiments are varying the antifouling paint and the pumping systems for the SeaBird Microcats. Current Global Drifter Program plans include the deployment of SVP-Microcat pairs in the Bay of Biscay west of France, each pair consisting of one drifter with pumping and one without, with sequential recoveries to evaluate the success and necessity of pumping. In the future, these observations will provide calibration and validation for satellite-derived sea surface salinity products.

Subsurface temperature: Several drifter manufacturers are developing drifters with thermistor chains to measure temperature profiles of the ocean's upper O(100 m). These observations would be invaluable for measuring mixed layer heat content variability, which can be poorly correlated with SST changes (Kelly, 2004).

6. Recent drifter-based studies: an overview

A large number of studies have used drifter observations to map currents and their variability in various regions. Recent examples (2000–present) have focused on the North Atlantic (Flatau et al., 2003), Labrador Sea (Cuny et al., 2002), Caribbean Sea (Centurioni and Niiler, 2003; Richardson, 2004), subtropical eastern Atlantic (Zhou et al., 2000), tropical Atlantic (Grodsky and Carton, 2002; Lumpkin and Garzoli, 2005), eastern South Atlantic (Largier and Boyd, 2001), tropical Pacific (Grodsky and Carton, 2001b; Johnson, 2001; Yaremchuk and Qu, 2004), central subtropical Pacific (Lumpkin and Flament, 2001; Flament et al., 2001), western Pacific (Niiler et al., 2003), North Pacific (Rabinovich and Thomson, 2001), tropical Indian (Grodsky and Carton, 2001a) and Southern (Zhou et al., 2002) oceans. Several recent studies have also focused on marginal seas including the Japan/East (Lee et al., 2000), South China (Centurioni et al., 2004) and Black (Poulain et al., 2004; Zhurbas et al., 2004) seas.

Because drifters follow the two-dimensional surface flow, they are ideal for studying the dispersion of surface particles such as fish larvae and other plankton and buoyant pollutants such as oil spills. Their observations of dispersion can also be used to quantify the effect of mesoscale variability upon mean transports (c.f. Davis, 1991). Early studies of oceanic dispersion from drifter observations (Richardson, 1983; Davis, 1985; Krauss and Böning, 1987) addressed the relevance of Taylor's (1921) classical dispersion theory. Taylor demonstrated that the mean square distance that a particle will diffuse can be characterized in a homogeneous, stationary field of eddies by time and length scales known as the Lagrangian integral scales. These are in principle different from their Eulerian counterparts, although some mixing length-based studies have mapped eddy diffusivities using observations of Eulerian length scales (e.g., Stammer, 1998). Lumpkin et al. (2002) compared the Lagrangian and Eulerian length scales from surface drifters and altimetry, and found that they were proportional only in the most energetic parts of the ocean (such as the Gulf Stream) where Lagrangian particles are advected around eddies at time scales much shorter than the Eulerian time scale. In the tropical Pacific, Bauer et al. (2002) separated mean and eddy drifter velocities using optimized bicubic splines and found that eddy diffusivity in this region is strongly anisotropic: zonal diffusion is up to seven times larger than meridional diffusion, due to parcel trapping in coherent features such as equatorial and tropical instability waves (Bauer et al., 2002). More recently, Zhurbas and Oh (2004) mapped the global surface diffusivity using a methodology designed to avoid contaminating eddy statistics by time-mean flow shear. Their maps of apparent diffusivity revealed enhanced values in zonal bands at $\sim 30^\circ$ in both southern and northern hemispheres. They attributed this to meandering, eddy-rich eastward currents in the North Atlantic (Azores Current) and North Pacific (North Subtropical

Countercurrent), and to the westward drift of Agulhas retroflection eddies in the South Atlantic. In the South Pacific, they argued that the distribution indicated the presence of a South Subtropical Countercurrent.

Eddy statistics from SVP drifter observations can be compared to those of simulated drifters in general circulation models, in order to assess how well the eddy-resolving models simulate near-surface turbulence and associated Lagrangian scales. This type of analysis has shown that the 1/12°-resolution Miami Isopycnic Coordinate Ocean Model (MICOM) underestimates EKE in the Gulf Stream extension and ocean interior, perhaps due to the climatological forcing employed or the lack of vertical shear in the bulk mixed layer (Garraffo et al., 2001). Similarly, the 1/10°-resolution Parallel Ocean Program (POP) model does not reproduce the observed Lagrangian scales, due to the model being too hydrodynamically stable in the surface layer (McClean et al., 2002).

Drifter observations of current and SST are also extremely valuable when evaluating the role of oceanic processes in SST variations. These data have been used to show that tropical instability waves, zonal advection, storage and entrainment all play a major role in the heat budget of the Pacific (Hansen and Paul, 1987; Swenson and Hansen, 1999) and Atlantic (Foltz et al., 2003) equatorial cold tongues.

A number of methodological advances have been published recently, adding value to the SVP drifter data set. For example, as noted earlier, many observations have been collected by non-SVP drifters, including the dense data set collected by FGGE drifters in the Southern Ocean. Recently, Pazan and Niiler (2004) announced a data set of ocean currents derived by combining these data after applying a drifter-dependent slip correction model (Pazan and Niiler, 2001). The types of drifters in this data set include SVP (both with and without drogue), FGGE (including later FGGE-type drifters deployed by the International Ice Patrol), and Navy-AN/WSQ-6.

Many oceanic regions have been sampled very heavily in some times of the year and lightly at other times, due to infrequent batch deployments from research vessels or ships of opportunity. In regions with strong seasonal fluctuations, such as the tropical Atlantic, this will produce biased estimates of the mean flow when the data are averaged in bins. Lumpkin (2003) addressed this problem by dividing the Lagrangian time series into spatial bins and, within each bin, decomposing the time series into time-mean, annual and semiannual harmonics, and a residual. This decomposition was performed using a Gauss-Markov technique familiar in the oceanographic literature for its use in box inverse models (e.g.. Ganachaud and Wunsch, 2000). This approach can resolve the amplitudes and phases of seasonal fluctuations throughout most of the tropical Atlantic basin with the present density of SVP drifter observations (Lumpkin and Garraffo, 2005).

An extremely exciting recent development is the synthesis of SVP drifter observations and satellite altimetry. Altimetry is excellent at capturing the variations of sea level height associated with geostrophic velocity anomalies, but cannot yet map absolute sea level with sufficient accuracy to resolve time-mean currents. Furthermore, sea level anomaly fails to account for significant ageostrophic components of velocity variation, such as centrifugal effects that may account for differences in drifter-derived and altimeter-derived eddy kinetic energy (EKE) on either side of the Gulf Stream front (Fratantoni, 2001). In addition, gridded altimetric products smooth the observations and thus tend to systematically underestimate EKE. Niiler et al. (2003) describe a methodology to synthesize Ekman-removed drifter speeds with gridded altimetric velocity anomalies in regions where they are significantly correlated. This methodology uses concurrent drifter and altimetry velocities in order to calibrate the altimetry, making its amplitude consistent with the in-situ observations, and uses the continuous time series from altimetry to correct for biased drifter sampling of mesoscale to interannual variations. By applying this approach to the global data set of drifter observations, Niiler et al. (2004a) have produced a map of the absolute sea level of the global ocean for the period 1992–2002. In a similar study, Rio and Hernandez (2004) synthesized a geoid model, operational winds, and observations from drifters, altimetry, and hydrography to produce an alternative global mean dynamic topography (Rio and Hernandez, 2004). Future work will improve upon these efforts by using results from the Gravity Recovery and Climate Experiment (GRACE) and the rapidly growing data sets of Argo float profiles and drifter trajectories in remote regions such as the Southern Ocean.

7. The future

The design of the SVP drifter has clearly not ceased to evolve – exemplified by the recent introduction of the mini drifter – while its qualitative characteristics and water-following properties have remained relatively steady since the earliest deployments. Incremental improvements in design and manufacturing will continue to increase drifter lifetime, and alternative methods for detecting drogue presence (such as tether strain) are being considered. New methodologies for drifter data analysis will continue to be developed, aided by increasing information from the ever-growing drifter array and from other sources of complimentary observations. Dense deployments in eddy-rich, frontal regions will help us improve our understanding of eddy fluxes and their role in modifying air-sea heat fluxes and water mass formation.

The quality of drifter data will also improve with updated interpolation schemes. As noted by Hansen and Poulain (1996), the structure functions used in the kriging interpolation are derived from tropical Pacific observations and assume uncorrelated zonal and meridional speeds. At high latitudes, these velocity components are often correlated due to looping motion in mesoscale eddies and inertial oscillations. Future interpolation schemes might exploit Lagrangian stochastic models with spin (e.g., Reynolds, 2002) which can include this behavior. Hansen and Poulain (1996) considered a structure function for velocity which was consistent with diffusion, but found that the total (as opposed to eddy, or turbulent) velocity was not robustly interpolated. At the present density of drifter observations, seasonal climatologies of near-surface currents can be mapped at sufficient density to ameliorate this problem. Revised interpolation approaches will provide better error estimates of the interpolated positions and velocity, and may allow improved estimates of the Lagrangian acceleration $D\boldsymbol{u}/Dt$.

By September 2005 the surface drifting buoy array of NOAA's Global Ocean Observing System and Global Climate Observing System is projected to consist of 1250 SVP drifters at a nominal global resolution of $5^\circ \times 5^\circ$. The major challenge facing AOML's Global Drifter Center (GDC), which coordinates drifter deployments, is to arrange deployments in regions of surface divergence and areas infrequently visited by research or volunteer observation vessels. This logistical challenge is being addressed by air deployments, increased international cooperation, and the development of tools to predict global drifter array coverage based on its present distribution and historical advection/dispersion. As the array grows, it provides invaluable observations of ocean dynamics, meteorological conditions and climate variations, and offers a platform to test experimental sensors measuring surface conductivity, rain rates, biochemical concentrations, and air-sea fluxes throughout the world's oceans.

Acknowledgements. The authors would like to thank the worldwide group of Global Drifter Program operational partners, whose contributions have established a truly global array of surface drifters. We would like to acknowledge Craig Engler, Jessica Redman and Erik Valdes for their frequent assistance. Discussions with Jeff Wingenroth and Sergey Motyzhev were extremely valuable. We thank Peter Niiler for many enlightening conversations, and for his comments on an early draft of this chapter which helped improve it tremendously. Additional comments by Claudia Schmid, Sang-Ki Lee and two anonymous reviewers were also valuable. NCEP Reanalysis 2 data are provided by the NOAA-CIRES Climate Diagnostics Center, Boulder, Colorado from their Web site at http://www.cdc.noaa.gov/. This work was funded by NOAA's Office of Global Programs and the Atlantic Oceanographic and Meteorological Laboratory.

References

Argos, 1996: Argos user manual 1.0. Technical report, CLS, Toulouse, France.

Bauer, S., M. Swenson, and A. Griffa, 2002: Eddy-mean flow decomposition and eddy diffusivity estimates in the tropical Pacific Ocean. 2. Results. *J. Geophys. Res.*, **107**, 3154–3171.

Bograd, S. J., A. B. Rabinovich, R. E. Thomson, and A. J. Eert, 1999: On sampling strategies and interpolation schemes for satellite-tracked drifters. *J. Atmos. Oceanic Technol.*, **16**, 893–904.

Centurioni, L. R. and P. P. Niiler, 2003: On the surface currents of the Caribbean Sea. *Geophys. Res. Letters*, **30**, 1279, doi:10.1029/2002GL016231.

Centurioni, L. R., P. P. Niiler, and D. K. Lee, 2004: Observations of inflow of Philippine Sea water into the South China Sea through the Luzon Strait. *J. Phys. Oceanogr.*, **34**, 113–121.

Cuny, J., P. B. Rhines, P. P. Niiler, and S. Bacon, 2002: Labrador Sea boundary currents and the fate of the Irminger Sea Water. *J. Phys. Oceanogr.*, **32**, 627–647.

Davis, R., 1985: Drifter observations of coastal surface currents during CODE: The statistical and dynamical views. *J. Geophys. Res.*, **90**, 4756–4772.

— 1991: Observing the general circulation with floats. *Deep Sea Res.*, **38**, S531–S571.

Ekman, V. W., 1905: On the influence of the Earth's rotation on ocean currents. *Ark. Mat. Astron. Fys.*, **2**, 1–52.

Flament, P. J., R. Lumpkin, J. Tournadre, R. Kloosterziel, and L. Armi, 2001: Vortex pairing in an unstable anticyclonic shear flow: discrete subharmonics of one pendulum day. *J. Fluid Mech.*, **440**, 401–410.

Flatau, M. K., L. Talley, and P. P. Niiler, 2003: The North Atlantic Oscillation, surface current velocities, and SST changes in the subpolar North Atlantic. *J. Climate*, **16**, 2355–2369.

Foltz, G. R., S. A. Grodsky, J. A. Carton, and M. J. McPhaden, 2003: Seasonal mixed layer heat budget of the tropical Atlantic Ocean. *J. Geophys. Res.*, **108**, 3146, doi:10.1029/2002JC001584.

Franklin, B., 1785: Sundry marine observations. *Trans. Am. Philos. Soc., Ser. 1*, **2**, 294–329.

Fratantoni, D. M., 2001: North Atlantic surface circulation during the 1990's observed with satellite-tracked drifters. *J. Geophys. Res.*, **106**, 22067–22093.

Fulton, T. W., 1897: The surface currents of the North Sea. *Scottish Geographical Mag.*, **13**, 636–645.

Ganachaud, A. S. and C. Wunsch, 2000: Improved estimates of global ocean circulation, heat transport and mixing from hydrographic data. *Nature*, **408**, 453–457.

Garraffo, Z., A. J. Mariano, A. Griffa, C. Veneziani, and E. Chassignet, 2001: Lagrangian data in a high resolution numerical simulation of the North Atlantic. I: Comparison with *in-situ* drifter data. *J. Mar. Sys.*, **29**, 157–176.

Garrett, J. F., 1980: The availability of the FGGE drifting buoy system data set. *Deep Sea Res.*, **27**, 1083–1086.

Geyer, W. R., 1989: Field calibration of mixed-layer drifters. *J. Atmos. Oceanic Technol.*, **6**, 333–342.

Grodsky, S. A. and J. A. Carton: 2001a, Anomalous surface currents in the tropical Indian Ocean. *Geophys. Res. Letters*, **28**, 4207–4210.

— 2001b: Intense surface currents in the Tropical Pacific during 1996-1998. *J. Geophys. Res.*, **106**, 16,673–16,684.

— 2002: Surface drifter pathways originating in the equatorial Atlantic cold tongue. *Geophys. Res. Letters*, **29**, 10,1029–10,1041.

Hansen, D. and A. Herman, 1989: Temporal sampling requirements for surface drifting buoys in the tropical Pacific. *J. Atmos. Oceanic Technol.*, **6**, 599–607.

Hansen, D. and P.-M. Poulain, 1996: Quality control and interpolations of WOCE-TOGA drifter data. *J. Atmos. Oceanic Technol.*, **13**, 900–909.

Hansen, D. V. and C. A. Paul, 1987: Vertical motion in the eastern equatorial Pacific inferred from drifting buoys. *Oceanol. Acta*, **6**, 27–32.

Johnson, G. C., 2001: The Pacific Ocean subtropical cell surface limb. *Geophys. Res. Letters*, **28**, 1771–1774.

Kelly, K. A., 2004: The relationship between oceanic heat transport and surface fluxes in the western North Pacific. *J. Climate*, **17**, 573–588.

Kennan, S., P. P. Niiler, and A. Sybrandy, 1998: Advances in drifting buoy technology. *International WOCE Newsletter*, **30**, 7–10.

Kessler, W. S. and B. A. Taft, 1987: Dynamic heights and zonal geostrophic transports in the central tropical Pacific during 1979-1984. *J. Phys. Oceanogr.*, **17**, 97–122.

Krauss, W. and C. Böning, 1987: Lagrangian properties of eddy fields in the northern North Atlantic as deduced from satellite-tracked buoys. *J. Mar. Res.*, **45**, 259–291.

Largier, J. and A. J. Boyd, 2001: Drifter observations of surface water transport in the Benguela Current during winter 1999. *South African Journal of Science*, **97**, 223–229.

Lee, D.-K., P. P. Niiler, S.-R. Lee, K. Kim, and H.-J. Lie, 2000: Energetics of the surface circulation of the Japan/East Sea. *J. Geophys. Res.*, **105**, 9561–19573.

Letelier, R., M. Abbott, and D. Karl, 1996: Southern Ocean optical drifter experiment. *Antarctic Journal of the United States*, **30**, 108–110.

Levitus, S., 1982: Climatological atlas of the world ocean. *NOAA Professional Paper. U. S. Dept of Commerce National Oceanic and Atmospheric Administration*, **13**, 173.

Lumpkin, R., 2003: Decomposition of surface drifter observations in the Atlantic Ocean. *Geophys. Res. Letters*, **30**, 1753, 10.1029/2003GL017519.

Lumpkin, R. and P. Flament, 2001: Lagrangian statistics in the central North Pacific. *J. Mar. Sys.*, **29**, 141–155.

Lumpkin, R. and Z. Garraffo, 2005: Evaluating the decomposition of Tropical Atlantic drifter observations. *J. Atmos. Oceanic Technol.*, **22**, 1403–1415.

Lumpkin, R. and S. L. Garzoli, 2005: Near-surface circulation in the tropical Atlantic Ocean. *Deep Sea Res., Part I*, **52**, 495–518, 10.1016/j.dsr.2004.09.001.

Lumpkin, R., A.-M. Treguier, and K. Speer, 2002: Lagrangian eddy scales in the northern Atlantic Ocean. *J. Phys. Oceanogr.*, **32**, 2425–2440.

McClean, J. L., P.-M. Poulain, J. W. Pelton, and M. E. Maltrud, 2002: Eulerian and Lagrangian statistics from surface drifters and a high-resolution POP simulation of the North Atlantic. *J. Phys. Oceanogr.*, **32**, 2472–2491.

McNally, G. J., W. C. Patzert, J. A D Kirwan, and A. C. Vastano, 1983: The near-surface circulation of the North Pacific using satellite tracked drifting buoys. *J. Geophys. Res.*, **88**, 7634–7640.

Milliff, R. F., P. P. Niiler, J. Morzel, A. E. Sybrandy, D. Nychka, and W. G. Large, 2003: Mesoscale correlation length scales from NSCAT and Minimet surface wind retrievals in the Labrador Sea. *J. Atmos. Oceanic Technol.*, **20**, 513–533.

Nath, J. H., 1977: Wind tunnel tests on drogues. Technical report, NOAA Data Buoy Office.

Niiler, P., 2001: The world ocean surface circulation. *Ocean Circulation and Climate*, G. Siedler, J. Church, and J. Gould, eds., Academic Press, volume 77 of *International Geophysics Series*, 193–204.

Niiler, P. P., 2003: A brief history of drifter technology. *Autonomous and Lagrangian Platforms and Sensors Workshop*, Scripps Institution of Oceanography, La Jolla, California.

Niiler, P. P., R. Davis, and H. White, 1987: Water-following characteristics of a mixed-layer drifter. *Deep Sea Res.*, **34**, 1867–1882.

Niiler, P. P., N. A. Maximenko, and J. C. McWilliams: 2004a, Dynamically balanced absolute sea level of the global ocean derived from near-surface velocity observations. *Geophys. Res. Letters*, **30**, 2164, doi:10.1029/2003GL018628.

Niiler, P. P., N. A. Maximenko, G. G. Panteleev, T. Yamagata, and D. B. Olson: 2003, Near-surface dynamical structure of the Kuroshio Extension. *J. Geophys. Res.*, **108**, 3193, doi:10.1029/2002JC001461.

Niiler, P. P. and J. D. Paduan, 1995: Wind-driven motions in the northeast Pacific as measured by Lagrangian drifters. *J. Phys. Oceanogr.*, **25**, 2819–2830.

Niiler, P. P., W. Scuba, and D.-K. Lee: 2004b, Performance of Minimet wind drifters in Hurricane Fabian. *The Sea, Journal of the Korean Society of Oceanography*, **9**, 7pp.

Niiler, P. P., A. Sybrandy, K. Bi, P. Poulain, and D. Bitterman, 1995: Measurements of the water-following capability of holey-sock and TRISTAR drifters. *Deep Sea Res.*, **42**, 1951–1964.

Pazan, S. E. and P. P. Niiler, 2001: Recovery of near-surface velocity from undrogued drifters. *J. Atmos. Oceanic Technol.*, **18**, 476–489.

— 2004: New global drifter data set available. *EOS*, **85**, 17.

Poulain, P.-M., R. Barbanti, S. Motyzhev, and A. Zatsepin, 2004: Statistical description of the Black Sea near-surface circulation using drifters in 1999-2003. *Deep Sea Res.*, **(submitted)**.

Rabinovich, A. B. and R. E. Thomson, 2001: Evidence of diurnal shelf waves in satellite-tracked drifter trajectories off the Kuril Islands. *J. Phys. Oceanogr.*, **31**, 2650–2668.

Ralph, E. A. and P. P. Niiler, 1999: Wind-driven currents in the Tropical Pacific. *J. Phys. Oceanogr.*, **29**, 2121–2129.

Reverdin, G., C. Frankignoul, E. Kestenare, and M. J. McPhaden, 1994: Seasonal variability in the surface currents of the equatorial Pacific. *J. Geophys. Res.*, **99**, 20323–20344.

Reynolds, A. M., 2002: On Lagrangian stochastic modeling of material transport in oceanic gyres. *Physica D*, **172**, 1442–1449.

Reynolds, R. W., N. A. Rayner, T. M. Smith, D. C. Stokes, and W. Wang, 2002: An improved in situ and satellite SST analysis for climate. *J. Climate*, **15**, 1609–1625.

Richardson, P., 1980: Gulf Stream ring trajectories. *J. Phys. Oceanogr.*, **10**, 90–104.

— 1983: Eddy kinetic energy in the North Atlantic from surface drifters. *J. Geophys. Res.*, **88**, 4355–4367.

— 2004: Caribbean current and eddies as observed by surface drifters. *Deep Sea Res.*, (in press).

Richardson, P. and G. Reverdin, 1987: Seasonal cycle of velocity in the Atlantic North Equatorial Countercurrent as measured by surface drifters, current meters, and ship drifts. *J. Geophys. Res.*, **92**, 3691–3708.

Richardson, P. and D. Walsh, 1986: Mapping climatological seasonal variations of surface currents in the Tropical Atlantic using ship drifts. *J. Geophys. Res.*, **91**, 10537–10550.

Richardson, P. L. and T. K. McKee, 1984: Average seasonal variation of the Atlantic equatorial currents from historical ship drift. *J. Phys. Oceanogr.*, **14**, 1226–1238.

Rio, M.-H. and F. Hernandez, 2003: High-frequency response of wind-driven currents measured by drifting buoys and altimetry over the world ocean. *J. Geophys. Res.*, **108**, 3283, doi:10.1029/2002JC001655.

— 2004: A mean dynamic topography computed over the world ocean from altimetry, in situ measurements, and a geoid model. *J. Geophys. Res.*, **109**, doi:10.1029/2003JC002226.

Stammer, D., 1998: On eddy characteristics, eddy transports, and mean flow properties. *J. Phys. Oceanogr.*, **28**, 727–739.

Sverdrup, H. U., M. W. Johnson, and R. H. Fleming, 1942: *The Oceans: their Physics, Chemistry and General Biology*. Prentice-Hall, Englewood Cliffs, N. J., 1087 pp.

Swenson, M. and D. V. Hansen, 1999: Tropical Pacific Ocean mixed layer heat budget: the Pacific Cold Tongue. *J. Phys. Oceanogr.*, **29**, 69–82.

Sybrandy, A. L. and P. P. Niiler, 1992: WOCE/TOGA Lagrangian drifter construction manual. WOCE Rep. 63, SIO Ref. 91/6, 58 pp., Scripps Inst. of Oceanogr., La Jolla, Calif.

Tait, J. B., 1930: The water drift in the northern and middle area of the North Sea and in the Faroe-Shetland Channel. Technical Report Scientific Investigation no. 4, Fishery Board for Scotland, Edinburgh.

Taylor, G., 1921: Diffusion by continuous movements. *Proc. Lond. Math. Soc.*, **20**, 196–212.

Thomson, C. W., 1877: *A Preliminary Account of the General Results of the Voyage of the HMS* Challenger. MacMillan, London.

Uda, M., 1935: The results of simultaneous oceanographical investigations in the North Pacific Ocean adjacent to Japan made in August, 1933. *Imperial Fisheries Exper. Sta. Journal*, **6**, 130 pp.

World Climate Research Program, 1988: WOCE surface velocity program planning committee report of first meeting: SVP-1 and TOGA pan-Pacific surface current study. WMO/TD-No.323, WCRP-26, 33 pp., World Meteorological Organization, Wormley.

Yaremchuk, M. and T. Qu, 2004: Seasonal variability of the large-scale currents near the coast of the Philippines. *J. Phys. Oceanogr.*, **34**, 844–855.

Zhou, M., P. P. Niiler, and J.-H. Hu, 2002: Surface currents in the Bransfield and Gerlache Straits, Antarctica. *Deep Sea Res., Part I*, **49**, 267–280.

Zhou, M., J. D. Paduan, and P. P. Niiler, 2000: Surface currents in the Canary Basin from drifter observations. *J. Geophys. Res.*, **105**, 21893–21911.

Zhurbas, V. and I. S. Oh, 2004: Drifter-derived maps of lateral diffusivity in the Pacific and Atlantic Oceans in relation to surface circulation patterns. *J. Geophys. Res.*, **109**, C05015, doi:10.1029/2003JC002241.

Zhurbas, V., A. G. Zatsepin, V. Yu, V. Grigoreva, V. N. Eremeev, V. V. Kremenetsky, S. V. Motyzhev, S. G. Poyarkov, P.-M. Poulain, S. V. Stanichny, and D. M. Soloviev, 2004: Water circulation and characteristics of currents of different scales in the upper layer of the Black Sea from drifter data. *Oceanology*, **44**, 30–43.

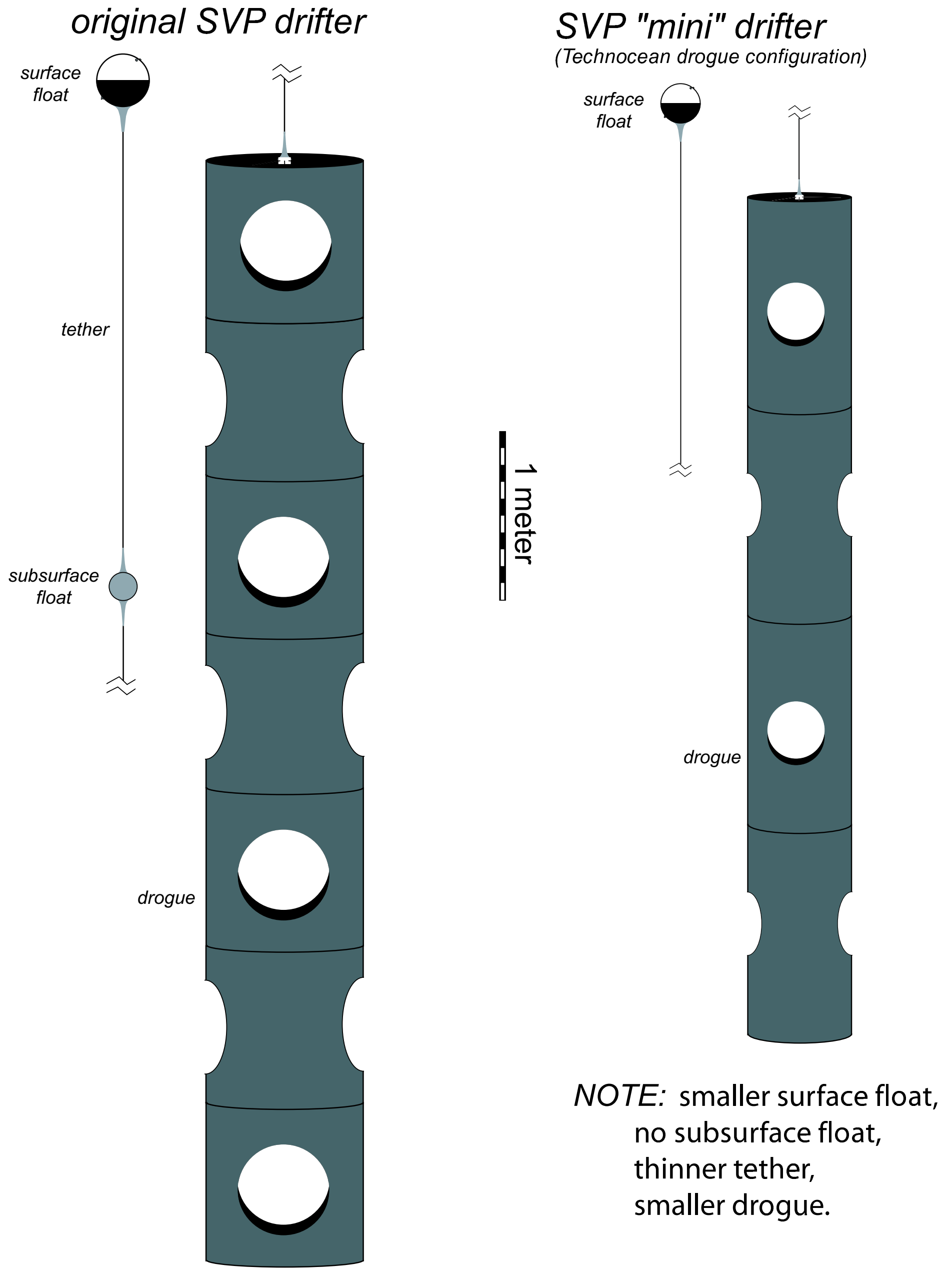

Figure 1: Schematic view of two SVP drifter types. All components are shown to scale; much of the tether length has been excluded. The drogues are centered at a depth of 15m.

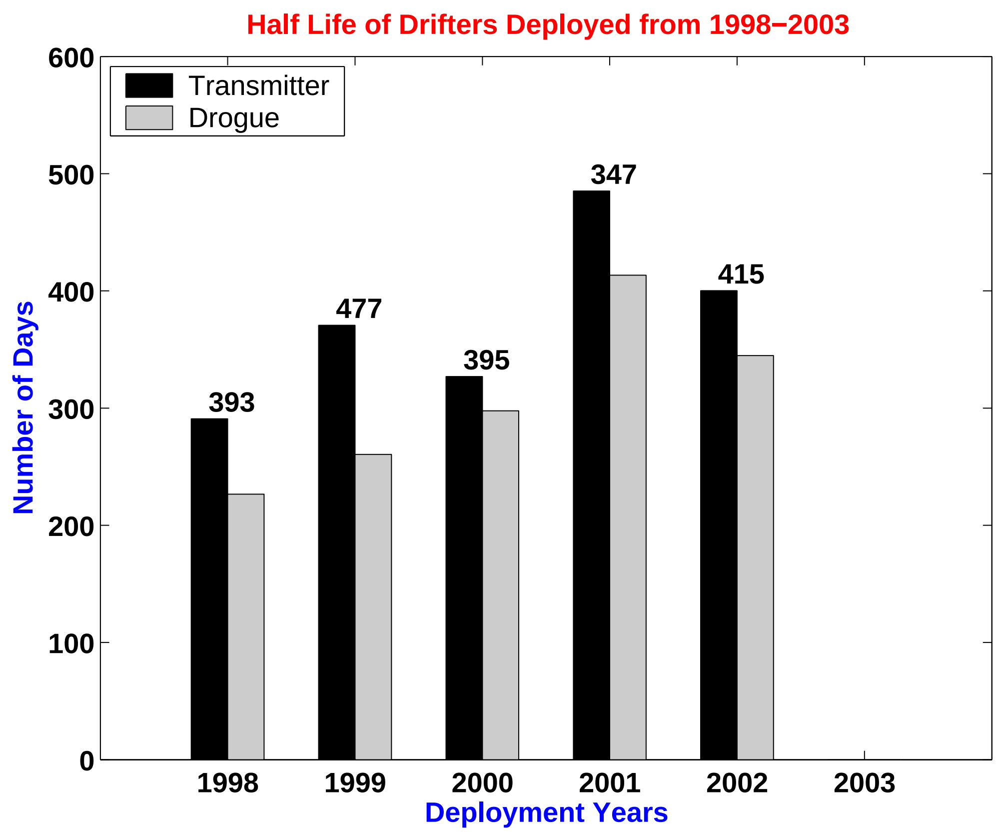

Figure 2: Half lives (days) of drifters deployed in 1998–2003. Black bar: half life of transmitter (e.g., velocity observations). Light grey bar: half life of drogued position observations. Numbers above the bars indicate how many drifters went into each calculation, e.g. how many drifters were deployed that year which did not run aground or were picked up. The 2003 half lives could not be determined because more than half are still alive and drogued.

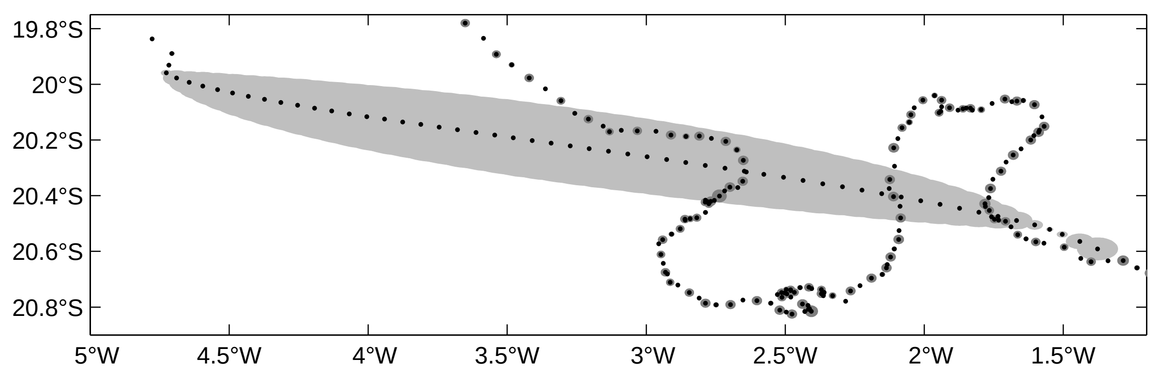

Figure 3: Interpolated locations of two drifters in the South Atlantic (black points), with shaded error bars from the kriging. For one of the drifters, 8–10 satellite fixes per day yields narrow error estimates (smaller than the black points for some quarter-day values). Transmissions from the other drifter were not picked up by the satellites for 12 days; interpolation through this gap yields a smooth trajectory and large location error estimates.

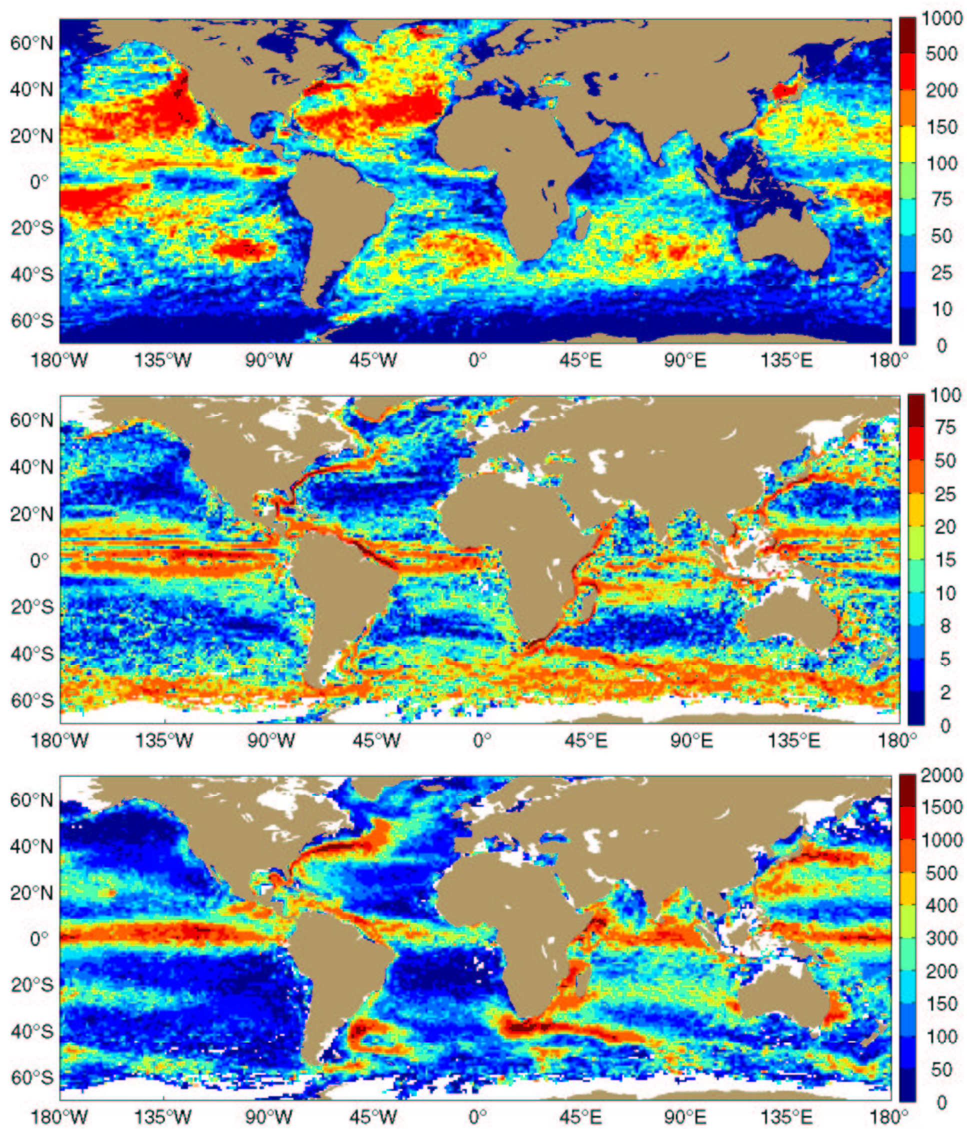

Figure 4: Fields calculated from the most recent decade (to 31 October 2004) of quality-controlled SVP drifter observations. *Top:* density of observations (drifter days per square degree). *Middle:* mean current speed (cm/s). *Bottom:* mean eddy kinetic energy (cm^2/s^2).

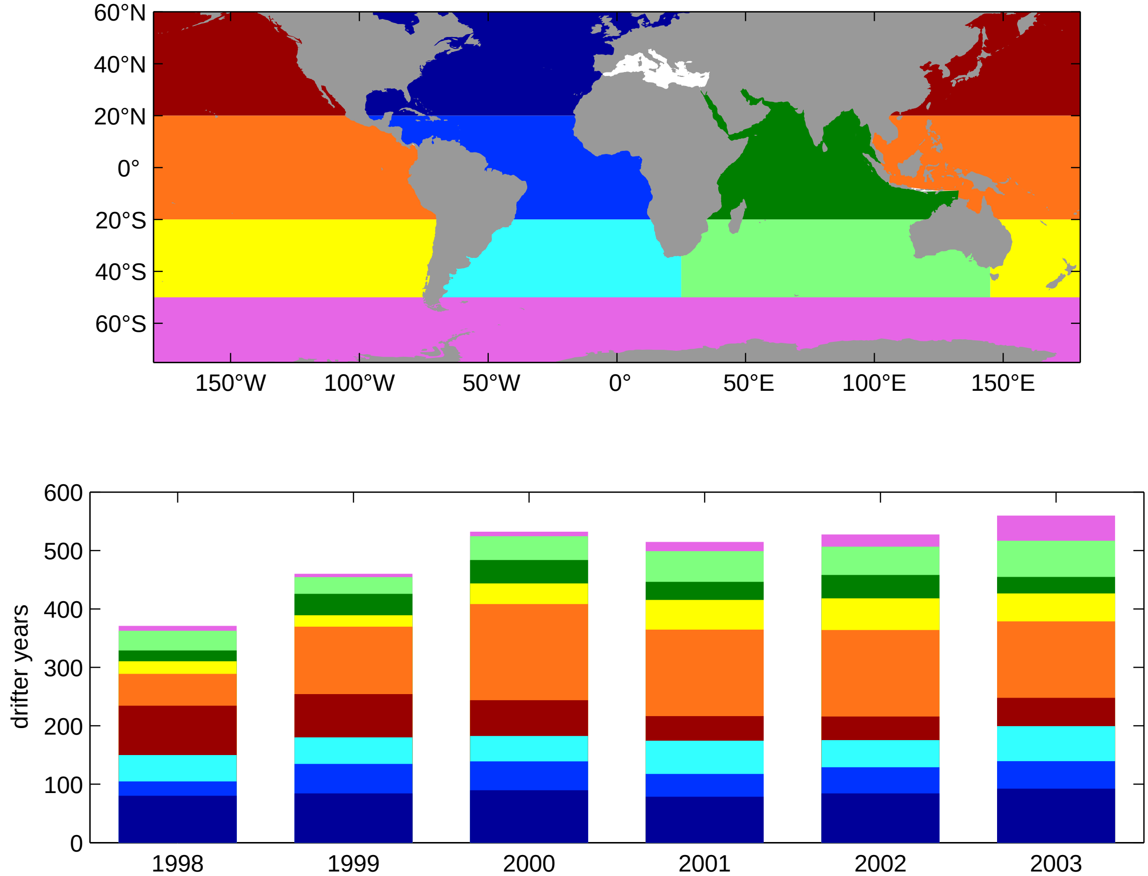

Figure 5: Top: regions (colored) used to subdivide data in bottom panel. Bottom: number of observations (drifter-years) per year in the different regions.

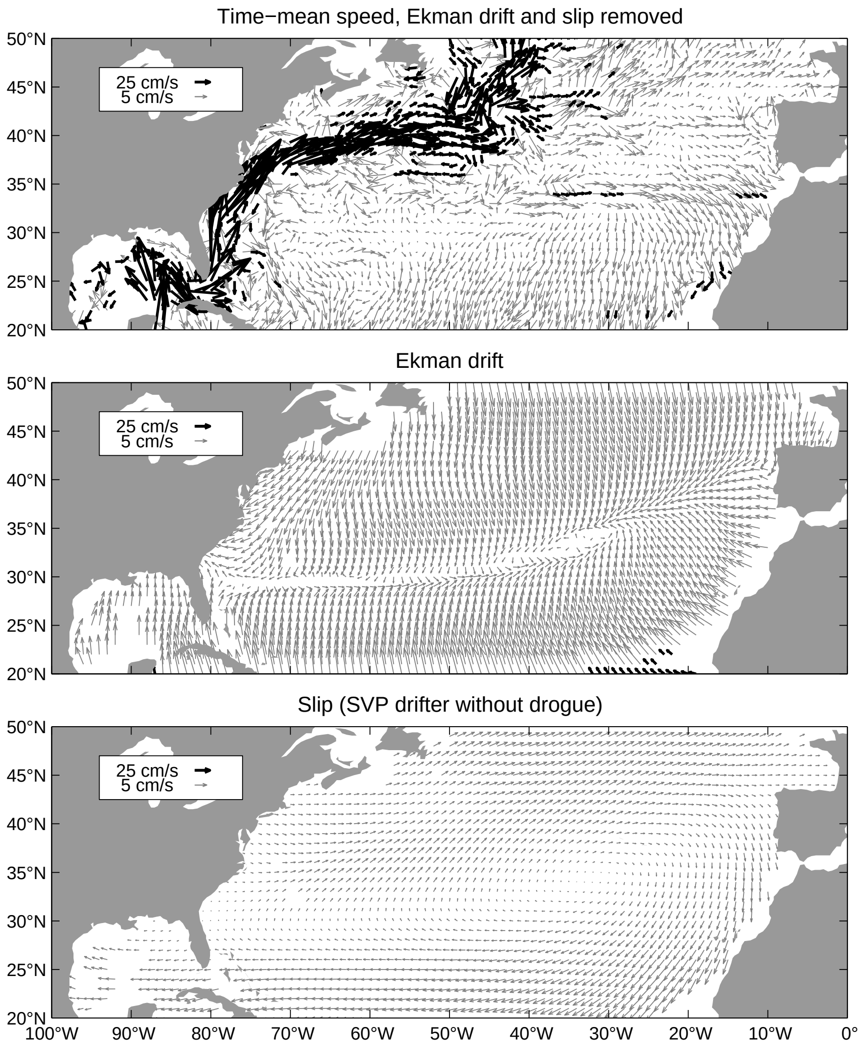

Figure 6: Top: Time-mean speed of all SVP drifters in the subtropical North Atlantic, October 1989 to April 2004, with Ekman drift and slip removed. A separate scale (bold arrows) is used for speeds exceeding 10 cm/s. Middle: time-mean Ekman drift (Ralph and Niiler, 1999; Niiler, 2001), showing the wind-driven convergence that forces the subtropical gyre (also see Fig. 15 of Rio and Hernandez, 2003). Bottom: time-mean slip of undrogued SVP drifters, using the parameterizations of Niiler and Paduan (1995) and Pazan and Niiler (2001). Drogued drifters experience a slip which is smaller by an order of magnitude. The total time-mean drift of undrogued drifters is given by the sum of these three panels.